Predicted energy band gaps of $(A^{III}B^{V})_{1-x}X^{IV}_{2x}$ metastable, substitutional, crystalline alloys

David W. Jenkins, Kathie E. Newman, and John D. Dow
Department of Physics, University of Notre Dame, Notre Dame, Indiana 46556
(Received 21 January 1985)

Predictions of the energy band gaps as functions of alloy composition are given for the Greene alloys, which are metastable, crystalline, substitutional alloys of III-V compounds and group-IV elemental materials. All possible combinations of these alloys involving Al, Ga, In, P, As, Sb, Si, Ge, and Sn are considered. The Γ and L conduction-band minima, relative to the valence-band maxima, exhibit characteristic V-shaped bowing and kinks as functions of composition x; the band edges at point X bifurcate at critical compositions corresponding to the order-disorder transition of Newman *et al.* The V-shaped bowing due to the transition offers the possibility of band gaps significantly smaller than expected on the basis of the conventional virtual-crystal approximation. Alloys with modest lattice mismatches that are predicted to have especially interesting band gaps include $(InP)_{1-x}Ge_{2x}$, $(AlSb)_{1-x}Sn_{2x}$, $(GaSb)_{1-x}Sn_{2x}$, and $(InAs)_{1-x}Sn_{2x}$, which are alloys with potentially small band gaps, and $(AlAs)_{1-x}Ge_{2x}$ and $(GaAs)_{1-x}Si_{2x}$, which are alloys with larger gaps and several interesting band-edge crossings as functions of composition.

I. INTRODUCTION

Recently, Greene and co-workers have fabricated a new class of semiconducting $(A^{III}B^{V})_{1-x}X^{IV}_{2x}$ alloys for a wide range of compositions.[1-4] The III-V compounds and group-IV elemental materials are normally immiscible at equilibrium,[5] but can be forced to mix by ion bombardment during growth. The resulting material, in the case of $(GaAs)_{1-x}Ge_{2x}$ or $(GaSb)_{1-x}Ge_{2x}$, is a metastable, crystalline, substitutional alloy with a lifetime at room temperature of order 10^{29} years.[6] The fundamental energy band gap of $(GaAs)_{1-x}Ge_{2x}$ has been determined from optical-absorption measurements and shows a nonparabolic V-shaped bowing as a function of alloy composition x (Ref. 7). A V-shaped band gap cannot be explained using the conventional virtual-crystal approximation, which gives approximately parabolic bowing. This V-shaped bowing is explained, however, with a zinc-blende-to-diamond, order-disorder phase transition.[8]

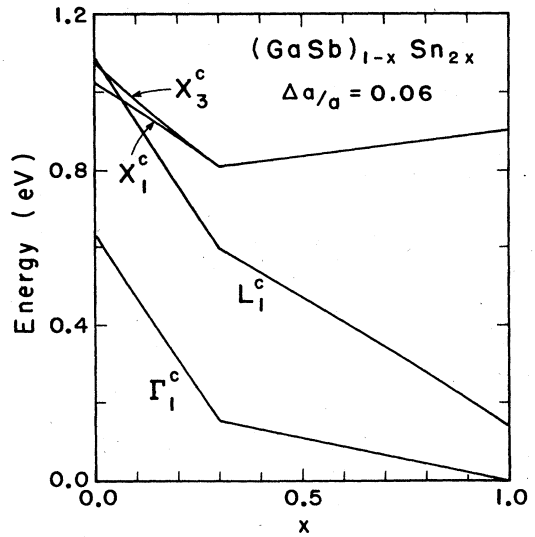

FIG. 1. Predicted band gaps at points Γ, L, and X versus alloy composition for $(GaSb)_{1-x}Sn_{2x}$. Kinks are seen in the Γ and L levels and the level at point X bifurcates at the assumed critical composition of Newman's zinc-blende-to-diamond phase transition, $x_c=0.3$. The gap is direct for all compositions, ranges from $\simeq 0.6$ to zero and decreases slowly as a function of composition from 0.15 eV to zero for compositions greater than the critical composition.

A theory for this transition has been developed by Newman *et al.*[8-10] and applied to $(GaAs)_{1-x}Ge_{2x}$. As seen in Fig. 1, where the theory is evaluated for the conduction-band minima near points Γ, L, and X for $(GaSb)_{1-x}Sn_{2x}$, the fundamental band gap exhibits a V-shaped bowing as a function of composition, with a kink at the critical composition x_c. This theory also gives smaller gaps than those of the conventional virtual-crystal approximation.

In this paper we apply this theory to the entire class of $(A^{III}B^{V})_{1-x}X^{IV}_{2x}$ alloys involving all possible combinations of Al, Ga, In, P, As, Sb, Si, Ge, and Sn, and we predict the energy band edges for these new metastable materials as functions of alloy composition x. We also establish general rules for understanding the chemical trends in the band gaps and for choosing a metastable $(A^{III}B^{V})_{1-x}X^{IV}_{2x}$ alloy with a desired energy band gap.

II. THEORY

The central idea of the present work is that all of the $(A^{III}B^{V})_{1-x}X^{IV}_{2x}$ metastable alloys should exhibit an order-disorder transition from an ordered zinc-blende structure (in which cations "know" which sites are supposed to be cation sites) to the disordered diamond structure in which there is no distinction between anion and cation sites. The critical composition x_c at which this tran-

sition occurs depends on the growth conditions of the alloy.

In developing a theory of the electronic structures of these alloys, we must remember that very little is presently known about these new and interesting materials. Many of the metastable alloys have not yet been grown; in most cases, satisfactory growth conditions are not yet known; and it is not yet definitely known if any of the Greene alloys other than $(GaSb)_{1-x}Ge_{2x}$ exhibits the order-disorder transition [which should be detected in x-ray diffraction as the disappearance of the (200) zinc-blende spot as x approaches x_c from below].[11] These facts are important in defining the nature of the theory that is appropriate at this time; it should be global and simple, rather than detailed and excessively quantitative. With this in mind, we assume both that all of the Greene alloys exhibit the Newman *et al.* transition, and that there exist growth conditions that will result in a critical composition $x_c=0.3$, the value appropriate for the two alloys grown to date by Greene and co-workers: $(GaAs)_{1-x}Ge_{2x}$ and $(GaSb)_{1-x}Ge_{2x}$ (x_c is probably experimentally adjustable).[12] We then predict the band structures (as functions of alloy composition x) of the remaining $(A^{III}B^{V})X^{IV}_{2x}$ metastable alloys with the intent of determining which alloys are likely to exhibit interesting and useful electronic structures—thereby targeting specific alloys for priority growth. Thus, we present these calculations in order to predict which materials are most likely to be interesting, rather than pretending to specify the band structures with any precision.

A. Order-disorder transition

The order-disorder transition involves a change of symmetry from the zinc-blende structure to the diamond-crystal structure. In this transition, the distinction between anion and cation sites is lost. The relevant order parameter is:[9]

$$M(x)=\langle P_{III}\rangle_{cation}-\langle P_{III}\rangle_{anion}\ , \tag{1}$$

where we imagine a zinc-blende lattice with sites labeled nominally "cation" and "anion," and $\langle P_{III}\rangle_{cation}$ is the average over all the lattice sites of the probability that a column-III atom occupies a nominal cation site. Thus $M(x)$ is proportional to the average electric dipole moment per unit cell. The order parameter depends on the growth conditions (e.g., substrate temperature, ion-bombardment energy) as well as on the composition x. For a completely ordered zinc-blende alloy, in which all column-III (column-V) atoms occupy nominal cation (anion) sites, we have $M=1-x$. If all the cations are on anion sites and the anions are on cation sites, we have merely mislabeled the nominal lattice and the order parameter is $x-1$. For the metastable ordered phase ($x<x_c=0.3$), we have $0<|M(x)|<1-x$. For the disordered diamond phase ($x>x_c$), we have $M=0$.

The theoretical problem posed by the Greene alloys is that of predicting the electronic structure of metastable alloys which are described by the order parameter $M(x)$. Thus, we must first execute a nonequilibrium phase-transition theory of $M(x)$ and then calculate the changes of the electronic structure as the alloys (with different composition x) undergo the order-disorder transition. Newman showed that this formidable problem could be solved by breaking it into four connected parts: (i) an equilibrium phase-transition theory of the order parameter $M(x)$, based on a three-component "spin"-Hamiltonian model similar to the Blume, Emery, Griffiths model[13] of He^3-He^4 solutions. [Spin-up, spin-down, or zero at a site in $(GaAs)_{1-x}Ge_{2x}$ signifies occupation of that site by Ga, As, or Ge, respectively.] (ii) Introduction of the nonequilibrium character of the alloys by eliminating those equilibrium phases that cannot be reached due to growth conditions (e.g., phase separation, which occurs at equilibrium, is prevented because characteristic growth times are small in comparison with the time required for the phases to diffuse apart); (iii) mutual elimination of two unknown parameters of the spin-Hamiltonian model, i.e., a spin-coupling constant J and an effective growth temperature T, in favor of one empirical parameter, the critical composition x_c;[14] and (iv) evaluation of the electronic structure using a modified virtual-crystal approximation and a tight-binding model[15] whose matrix elements depend parametrically on the order parameter $M(x;x_c)$. Thus, in the Newman approach there are two Hamiltonians: (i) a spin-Hamiltonian for treating the order-disorder transition and for calculating the order parameter $M(x;x_c)$ and (ii) an empirical tight-binding Hamiltonian—that depends parametrically on $M(x;x_c)$—for calculating the electronic structure.

B. Spin-Hamiltonian model

Newman *et al.* have shown that a III-V compound semiconductor such as GaAs can be modeled in a spin-Hamiltonian language as an "antiferromagnet" where spin-up or spin-down on a site represents occupation by a group-III atom or a group-V atom, respectively. Thus GaAs, with alternating Ga and As atoms, in this language, is an "antiferromagnet." The "magnetization" is proportional to the net electric dipole moment per unit cell, Eq. (1), and for zero-temperature GaAs at equilibrium, equals unity. In metastable $(A^{III}B^{V})_{1-x}X^{IV}_{2x}$ alloys, such as $(GaAs)_{1-x}Ge_{2x}$, occupation of a site by a column-IV atom such as Ge is represented by "spin" zero. If the Ge were to occupy both anion and cation sites without disturbing the occupation of these sites by Ga and As, then the order parameter would be $M(x)=1-x$. However, M is not $1-x$ because Ge (spin zero) dilutes the "magnetization" $M(x;x_c)$ of this "antiferromagnet," by removing nonzero "spins" at various sites, until there is insufficient "spin-spin" interaction for an average site to "know" it should have spin-up or spin-down. With a sufficient concentration x of dilutants (that depends on temperature), the "magnetization" vanishes, and the system undergoes a phase transition, from an "antiferromagnetic" zinc-blende state with $M\neq 0$ to an "unmagnetized" phase ($M=0$). That is, as Ge dilutes GaAs, an average cation site is no longer fully surrounded by As atoms and no longer feels electronically compelled to be occupied by a Ga atom rather than an As atom. The average electric dipole moment $M(x)$ of the ordered zinc-blende phase decreases and the system undergoes a transition from an ordered zinc-blende phase in which Ga atoms preferentially

occupy nominal cation sites to a disordered ($M=0$) diamond phase in which there is no distinction between anion and cation sites. Newman constructed a spin-Hamiltonian model of this order-disorder transition. The important physical parameter of this Hamiltonian is a nearest-neighbor spin coupling (which is related to energies of interaction of the pairs of atoms V-V, III-III, and III-V). The Hamiltonian, when treated in a mean-field approximation, yields the following equation for the order parameter $M(x;x_c)$:

$$\tanh[(M/(1-x_c)]=[M/(1-x)] , \quad (2)$$

where x_c is the critical composition of the order-disorder transition.

C. Tight-binding Hamiltonian

The electronic structure calculations are based on an empirical, ten-band, second-nearest-neighbor, tight-binding theory, which employs an sp^3s^* basis at each site of the zinc-blende lattice. The on-site and nearest-neighbor matrix elements of this model have been obtained previously by Vogl *et al.*,[15] who fit the known band structures of many III-V compounds and group-IV semiconductors. The Vogl matrix elements are augmented by one or two second-neighbor parameters[16] (see Table I) in order to obtain a better fit to the band structures of these semiconductors at the L point of the Brillouin zone. (The Vogl model was designed to fit the conduction-band structures well near points Γ and X.) The on-site matrix elements for these many semiconductors exhibit manifest chemical trends that depend only on the atomic energies of the atom on the site, to a good approximation. The off-diagonal nearest-neighbor matrix elements are inversely proportional to the square of the bond length d, according to the rule of Harrison *et al.*[17] For our purposes the important physical parameters of the tight-binding Hamiltonian are the on-site energies of the column-III, -IV, and -V atoms, which we shall interpolate using a generalized virtual-crystal approximation.[9] The on-site matrix elements are interpolated according to Eq. (3), as are Vd^2, where V is the off-diagonal matrix elements and d is the bond length of the alloy predicted by Vegard's law:[18] $d(x)=(1-x)d_{\text{III-V}}+xd_{\text{IV}}$.

We expect these $(A^{\text{III}}B^{\text{V}})_{1-x}X^{\text{IV}}_{2x}$ alloys to satisfy adequately the Onodera-Toyozawa[19] criterion for an "amalgamated" electronic spectrum, since the variations in on-site diagonal matrix elements are small in comparison with nearest-neighbor transfer matrix elements.[20] Therefore, we expect them to have relatively well-defined band structures which can be described (in a first approximation) by a mean-field theory of the virtual-crystal type. They cannot be treated with the ordinary virtual-crystal approximation, however, because (in the disordered "diamond" phase, in particular) they contain many antisite atoms (e.g., a column-III atom on a nominal anion site)—and the usual virtual-crystal approximation does not allow for antisite atoms. We circumvent this problem by using the generalized virtual-crystal approximation,[9] which has virtual anions and cations such that the virtual cation is (schematically):

$$[(1-x+M)/2]A^{\text{III}}+[(1-x-M)/2]B^{\text{V}}+xX^{\text{IV}} . \quad (3)$$

Here, A^{III}, X^{IV}, and B^{V} represent the column-III, -IV, and -V atoms, and $M(x;x_c)$ is the order parameter (1) of the order-disorder transition, obtained by solving Eq. (2).

TABLE I. Second-neighbor parameters. Note here that $\epsilon(p_xa,p_ya')=\epsilon(p_xc,p_yc')$ and $\epsilon(sa,p_xa)=\epsilon(p_xc,sc')$. See Ref. 16 for details.

Semiconductor	$\epsilon(sa,p_ya')$	$\epsilon(p_xa,p_ya')$
AlP	1.990	0.000
AlAs	1.830	−0.876
AlSb	0.101	0.000
GaP	0.641	0.000
GaAs	0.464	0.000
GaSb	0.688	0.000
InP	0.368	0.000
InAs	0.187	0.000
InSb	0.107	0.000
Si	0.000	0.146
Ge	0.157	0.000
Sn	0.000	0.056

III. RESULTS

The energies of the band edges (relative to the valence-band maximum, which is defined to be the zero of energy) are given in Fig. 1 for $(GaSb)_{1-x}Sn_{2x}$. Corresponding results for all possible $(A^{\text{III}}B^{\text{V}})_{1-x}X^{\text{IV}}_{2x}$ alloys are given in Figs. 2–4. The Γ conduction-band minimum occurs at $\mathbf{k}=(0,0,0)$ in the band structure. The edges labeled Δ and Λ refer to the conduction minima near the (1,0,0) and $(\frac{1}{2},\frac{1}{2},\frac{1}{2})$ points, respectively (i.e., near points X and L).[21] For $\mathbf{k}$ at the X point of the Brillouin zone, the conduction-band edge actually bifurcates as a function of alloy composition at the critical composition x_c, producing both an X_1 and an X_3 minimum in the zinc-blende (ordered) phase for $x<x_c$, but only one minimum for $x>x_c$ in the diamond (disordered) phase. This bifurcation is reflected in the dependence of the minima along the Δ line as functions of composition x (see Fig. 4), because these minima lie at wave vectors near point X. The relative minimum at point Γ, when plotted as a function of composition x, exhibits a kink at x_c, as does the band edge at the L point. The minimum in the Λ direction reflects the kinked behavior of the nearby L point.

In addition to the dependences on alloy composition x, there are discernible trends depending on the positions of the atoms in the Periodic Table. To facilitate quantification of these trends, we define an effective average atomic number:

$$\langle Z\rangle=xZ_{\text{IV}}+(1-x)(Z_{\text{III}}+Z_{\text{V}})/2 , \quad (4)$$

where, for example, Z_{III} is the atomic number of the column-III atom. Figure 5 shows that the Γ, Δ, and Λ band edges tend to decrease in energy with increasing

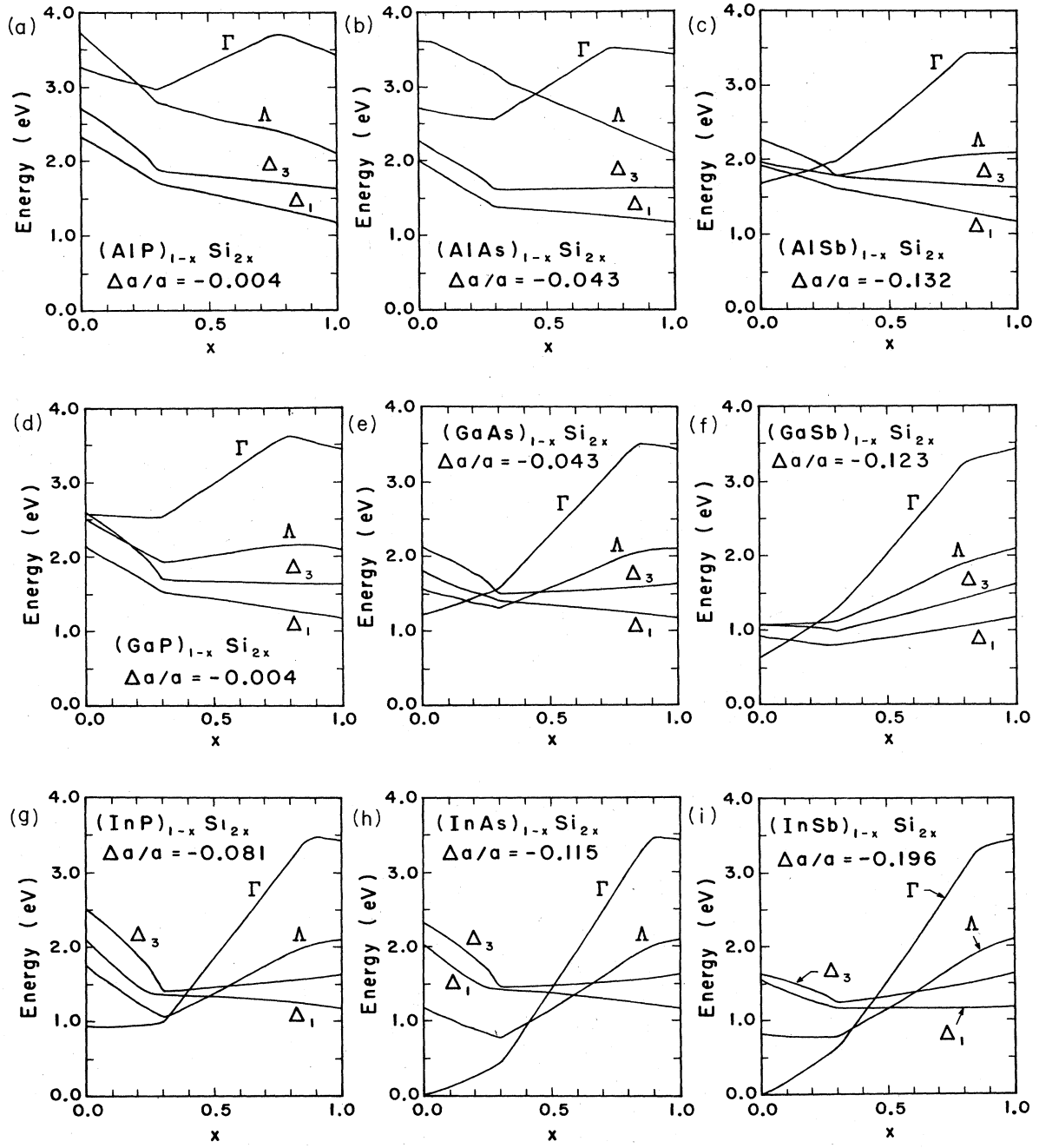

FIG. 2. Predicted band gaps of $(A^{III}B^{V})_{1-x}Si_{2x}$ alloys versus x, for the following III-V compounds: AlP, AlAs, AlSb, GaP, GaAs, GaSb, InP, InAs, and InSb. Lattice mismatches, defined by Eq. (5), are shown. Kinks can be seen in the Γ, Λ, and Δ levels at the assumed critical composition $x_c = 0.3$. The Δ minimum generally lies some distance from the X point in our tight-binding model, so the strict bifurcation at the X point is not clearly visible. The kinks near $x = 1$ are due to a crossing of the Γ_c^{15} and Γ_c^1 levels.

$\langle Z \rangle$, with Γ decreasing most rapidly and Δ decreasing least rapidly with $\langle Z \rangle$. This trend can be exploited, for example, to find metastable alloys with small fundamental band gaps for possible applications in infrared photography: The smaller gaps are associated with large average atomic numbers. Hence $(GaSb)_{1-x}Sn_{2x}$, with average atomic numbers ranging from 36.5 to 50, should be an interesting small-band-gap material, provided its electronic transport properties can be made suitable for device applications.

Predicted band gaps of the metastable zinc-blende-diamond Greene alloys fabricated from Al, Ga, In, P, As, Sb, Si, Ge, and Sn are shown in Figs. 2–4. General trends follow those of the prototypical alloy

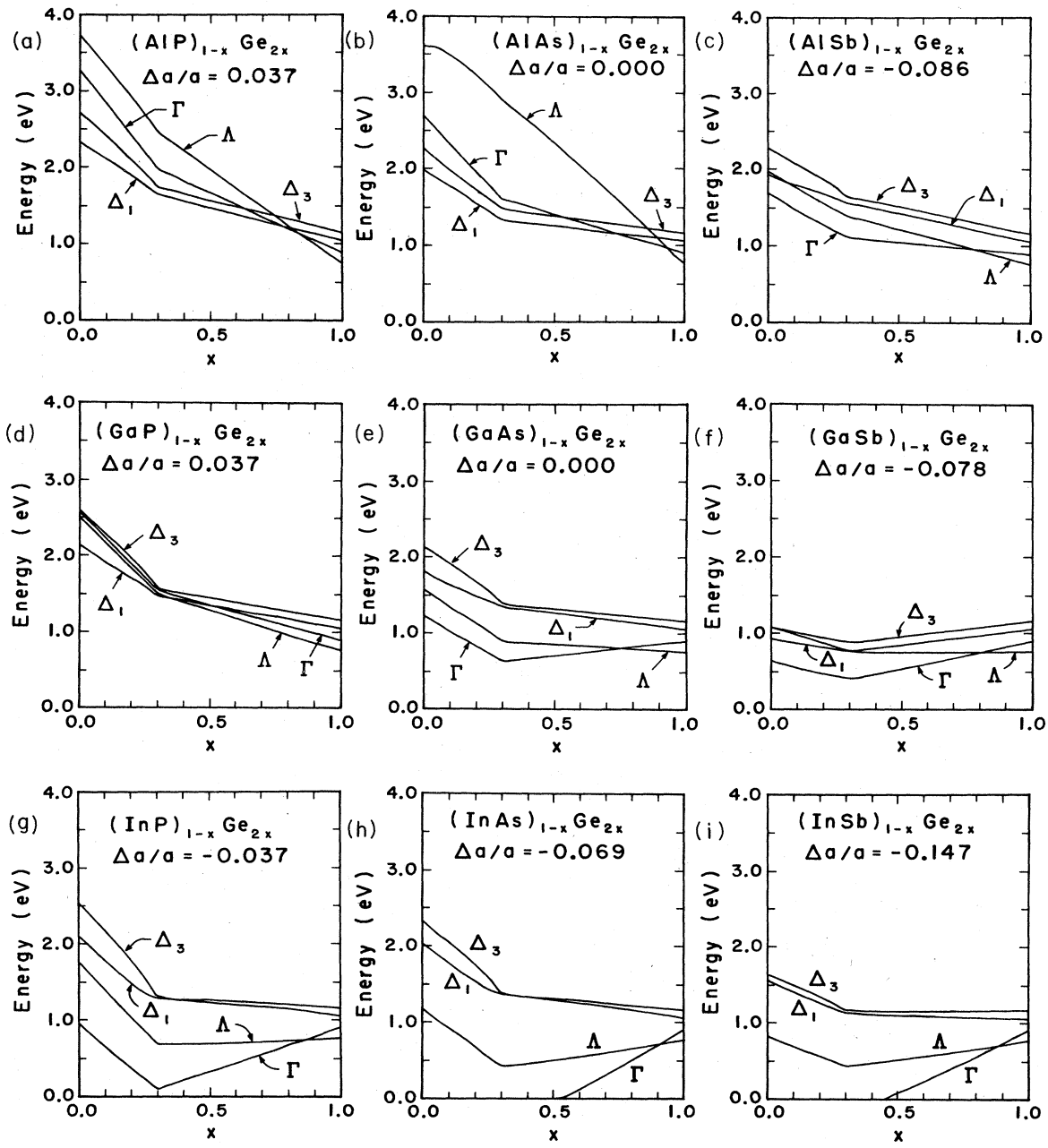

FIG. 3. Predicted band gaps of $(A^{III}B^{V})_{1-x}Ge_{2x}$ alloy versus x, for the following III-V compounds: AlP, AlAs, AlSb, GaP, GaAs, GaSb, InP, InAs, and InSb. Lattice mismatches, defined by Eq. (5), are shown. Kinks can be seen in all levels, at the assumed critical composition $x_c=0.3$. For some alloys, notably $(InP)_{1-x}Ge_{2x}$ for $x<0.4$ and $(InAs)_{1-x}Ge_{2x}$ for $x<0.5$, the Δ minimum occurs at the X point in our tight-binding model and the strict bifurcation at point X is clearly visible.

$(GaSb)_{1-x}Sn_{2x}$, shown in Fig. 1. All alloy band gaps exhibit kinks at x_c as a function of composition. There is always at least one kink in the minimum conduction-band edge at $x=x_c$, due to the phase transition. This kink is not associated with a crossing of the band edges, although these types of effects can also be seen at other compositions. For example, in $(InP)_{1-x}Ge_{2x}$ (Ref. 22) at $x=0.85$, the conduction band at Γ crosses with Λ and the alloy goes from being a direct-gap semiconductor to one with an indirect gap.

The alloys with the smallest lattice mismatches

$$\Delta a/a=(a_{IV}-a_{III\text{-}V})/a_{IV} \tag{5}$$

are especially interesting. We focus primarily on alloys with $\Delta a/a<0.07$. Values of $\Delta a/a$ are given in each figure.

Since the details of the band gaps for these alloys depend on the constituents, we summarize details below fig-

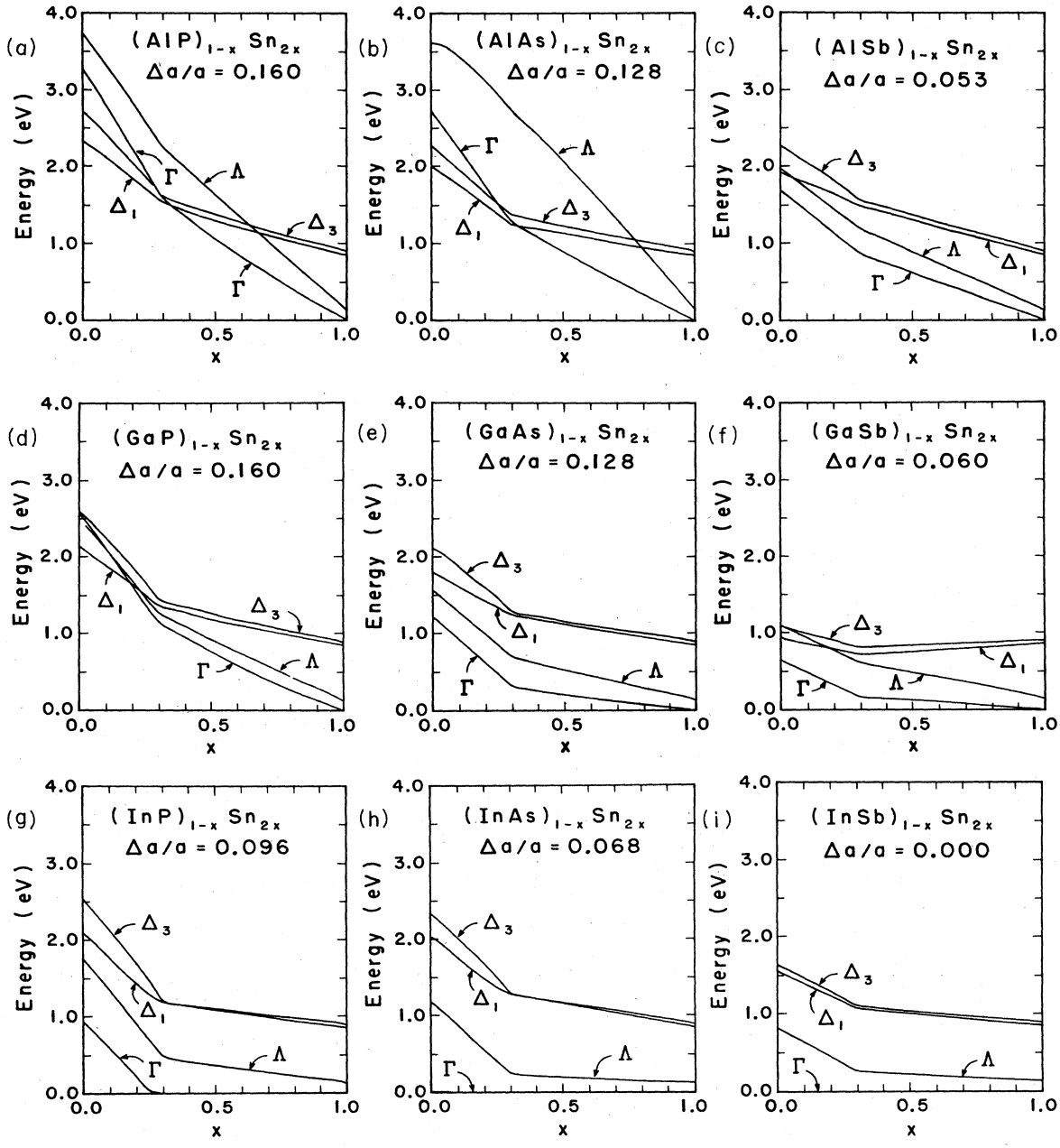

FIG. 4. Predicted band gaps of $(A^{III}B^{V})_{1-x}Sn_{2x}$ alloys versus x, for the following III-V compounds: AlP, AlAs, AlSb, GaP, GaAs, GaSb, InP, InAs, and InSb. Lattice mismatches, defined by Eq. (5), are shown. Kinks can be seen in all levels, at the critical composition $x_c = 0.3$. For some alloys, notably $(InP)_{1-x}Sn_{2x}$ for $x < 0.6$ and $(InAs)_{1-x}Sn_{2x}$ for $x < 0.5$, the Δ minimum occurs at the X point in our tight-binding model and the strict bifurcation at point X is clearly visible.

ure by figure. Figure 2 displays predicted band edges for zinc-blende materials combined in metastable alloys with Si. Those with the smallest lattice mismatches are $(AlP)_{1-x}Si_{2x}$ ($\Delta a/a = -0.004$), $(AlAs)_{1-x}Si_{2x}$ (-0.043), $(GaP)_{1-x}Si_{2x}$ (-0.004), and $(GaAs)_{1-x}Si_{2x}$ (-0.043).[23] Thus, of this class of well-lattice-matched alloys, one is restricted to materials with $\langle Z \rangle \leq 23$. The fundamental band gaps of these alloys vary from 1.17 eV for Si to 2.5 eV for ordinary AlP.[23] These gaps tend to have only one kink, at the critical composition $x = x_c$, because the fundamental gap, like that of Si, is along the Δ_1 line for all x, and does not cross Γ or Λ [the exception being $(GaAs)_{1-x}Si_{2x}$ for which we find crossings from Γ to Λ to Δ as a function of increasing composition]. The kink in Γ for $x \simeq 0.8$ is due to mixing of this level[23] and a Γ_c^{15} level not displayed (Si has $\Gamma_c^{15} < \Gamma_c^1$). In contrast to the small-lattice-mismatched materials, the heavily strained alloys (see the last row of Fig. 2), all show multiple band-

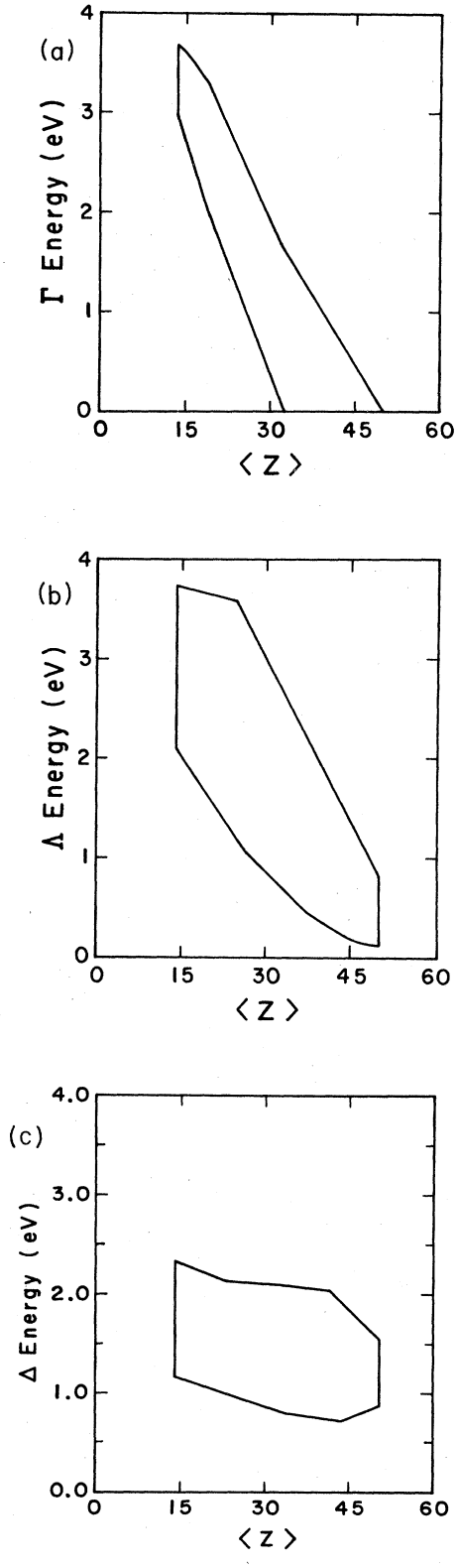

FIG. 5. Trends of the (a) Γ, (b) Λ, and (c) Δ band edges versus average atomic number $\langle Z \rangle$. The relevant energies for the $(A^{III}B^{V})_{1-x}X^{IV}_{2x}$ alloys in question lie within the boxes of the figures. Hence those at Γ and Λ, in particular, tend to decrease with increasing $\langle Z \rangle$.

edge crossings from Γ to Λ to Δ as a function of increasing composition x.

Figure 3 gives band edges for zinc-blende materials in metastable mixtures with Ge. Those with the smallest lattice mismatches are $(AlP)_{1-x}Ge_{2x}$ ($\Delta a/a = 0.037$), $(AlAs)_{1-x}Ge_{2x}$ (0.0), $(GaP)_{1-x}Ge_{2x}$ (0.037), $(GaAs)_{1-x}Ge_{2x}$ (0.0), and $(InP)_{1-x}Ge_{2x}$ (−0.037). In this class of alloys we are restricted to well-lattice-matched materials with $\langle Z \rangle \leq 32$. The band gaps of these alloys vary from 0.1 eV for $(InP)_{1-x}Ge_{2x}$ at $x = 0.3$ to 2.5 for ordinary AlP. The band gaps of these alloys have crossings from Δ to Γ to Λ for $(AlP)_{1-x}Ge_{2x}$ and $(AlAs)_{1-x}Ge_{2x}$ and from Γ to Λ for the others. Of the remaining alloys with larger mismatches, some, such as $(InAs)_{1-x}Ge_{2x}$ and $(InSb)_{1-x}Ge_{2x}$, have zero gap for some compositions x but, because the mismatch is larger, they may be difficult to grow.

Figure 4 presents our predictions for metastable alloys resulting from mixing zinc-blende materials with Sn. Those with the smallest lattice mismatches are $(AlSb)_{1-x}Sn_{2x}$ ($\Delta a/a = 0.053$), $(InAs)_{1-x}Sn_{2x}$ (0.068), $(GaSb)_{1-x}Sn_{2x}$ (0.060), and $(InSb)_{1-x}Sn_{2x}$ (0.0). In this class of alloys, lattice matching restricts us to materials with $32 \leq \langle Z \rangle \leq 50$. These are especially interesting materials because Sn has a zero band gap. The band gaps are predicted to be zero for the metastable alloys $(InAs)_{1-x}Sn_{2x}$ and $(InSb)_{1-x}Sn_{2x}$ for all compositions (despite the fact that the equilibrium compounds InAs and InSb have nonzero gaps[24]). All of the Sn-based metastable alloys (with small lattice mismatches) mentioned above are either direct-gap or zero-gap materials. $(GaSb)_{1-x}Sn_{2x}$ is particularly interesting, because the predicted gap varies from 0.15 eV to zero over a large range in composition, from 0.3 to 1.0. Hence, the gap is small and may not be too sensitive to fluctuations in local environment. This, along with $(InP)_{1-x}Ge_{2x}$, may be an especially good candidate for an infrared detector.[22] The remaining alloys, while covering a large range in gap size, from 2.5 eV for ordinary AlP to zero for Sn, all have large lattice mismatches, $\Delta a/a > 0.096$, and good-quality, long-lived, metastable samples of these materials may be difficult to grow.

IV. CONCLUSIONS

We have presented predictions of the energy band gaps versus alloy composition x for the Greene alloys: metastable, crystalline, substitutional alloys of III-V compounds and group-IV elemental materials. The band gaps at points Γ and L exhibit kinks and the X points bifurcate as functions of composition x, at a critical value x_c corresponding to the order-disorder transition of Newman *et al.* The V-shaped bowing offers the possibility of band gaps significantly smaller than expected on the basis of the conventional virtual-crystal approximation. Alloys with modest lattice mismatches that are predicted to have small band gaps include $(InP)_{1-x}Ge_{2x}$, $(AlSb)_{1-x}Sn_{2x}$, $(GaSb)_{1-x}Sn_{2x}$, and $(InAs)_{1-x}Sn_{2x}$. Larger band-gap alloys with several potentially interesting level crossings in the band gap include $(AlAs)_{1-x}Ge_{2x}$ and $(GaAs)_{1-x}Si_{2x}$.

ACKNOWLEDGMENTS

We gratefully acknowledge the generous support of the U.S. Army Research Office (Contract No. DAAG29-83-K-0122) and the U.S. Office of Naval Research (Contract Nos. N00014-77-C-0537 and N00014-84-K-0352). We thank J. E. Greene and S. Barnett for stimulating conversations about this work and their alloys.

[1]J. E. Greene, J. Vac. Sci. Technol. B **1**, 229 (1983).

[2]See also, Z. I. Alferov, R. S. Vantanyan, V. I. Korol'kov, I. I. Mokan, V. P. Ulin, B. S. Yavich, and A. A. Yakovenko, Fiz. Tekh. Poluprovodn. **16**, 887 (1982) [Sov. Phys. Semicond. **16**, 567 (1982)].

[3]A. J. Noreika and M. H. Francombe, J. Appl. Phys. **45**, 3690 (1974).

[4]P. Duwez, R. H. Williams, and W. Klement, Jr., J. Appl. Phys. **31**, 1500 (1960) were, to our knowledge, the first to grow some of these alloys for selected compositions.

[5]V. M. Glazov and V. S. Zemskov, *Physiochemical Principles of Semiconductor Doping* (IPST, Jerusalem, Israel, 1978). See also S. I. Shah, K. C. Cadien, and J. E. Greene, J. Electron. Mater. **11**, 53 (1980).

[6]K. C. Cadien, A. H. Eltoukhy, and J. E. Greene, Appl. Phys. Lett. **38**, 773 (1981); Vacuum **31**, 253 (1981).

[7]S. A. Barnett, M. A. Ray, A. Lastras, B. Kramer, J. E. Greene, P. M. Raccah, and L. L. Ables, Electron. Lett. **18**, 891 (1982). Typographical errors in the figures have been corrected in Ref. 8.

[8]K. E. Newman, A. Lastras-Martinez, B. Kramer, S. A. Barnett, M. A. Ray, J. D. Dow, J. E. Greene, and P. M. Raccah, Phys. Rev. Lett. **50**, 1466 (1983).

[9]K. E. Newman and J. D. Dow, Phys. Rev. B **27**, 7495 (1983).

[10]Equation (A17) of Ref. 9 is (obviously) misprinted and should read

$$4KzQ/(k_bT)=\ln[(1-x-Q)^2-M^2]/[(1-x+Q)^2-M^2]$$
$$+2\ln[(x-Q)/(x+Q)] .$$

[11]S. A. Barnett presented preliminary x-ray diffraction data for $(GaSb)_{1-x}Ge_{2x}$ indicating that this does indeed happen: Bull. Am. Phys. Soc. **29**, 203 (1984). See also, S. A. Barnett, B. Kramer, L. T. Romano, S. I. Shah, M. A. Ray, S. Fang, and J. E. Greene, *Layered Structure, Epitaxy, and Interfaces,* edited by J. M. Gibson and L. R. Dawson (North-Holland, Amsterdam, 1984).

[12]The critical composition x_c is bounded above by x_p, the percolation composition. An alternative theoretical description of $(GaAs)_{1-x}Ge_{2x}$ in terms of percolation, was given by M. I. D'yakonov and M. E. Raikn, Fiz. Tekh. Poluprovodn. **16**, 890 (1982) [Sov. Phys. Semicond. **16**, 570 (1982)]. However, percolation would produce a critical composition x_c near 0.6 not 0.3, as observed for $(GaAs)_{1-x}Ge_{2x}$. Preliminary x-ray diffraction studies (Ref. 11) favor the order-disorder model.

[13]M. Blume, V. J. Emery, and R. B. Griffiths, Phys. Rev. A **4**, 1071 (1971).

[14]Generally, neither J nor T is known, but both can be simultaneously eliminated from the equation for $M(x;x_c)$ if the phase-transition composition x_c is known. See Ref. 9.

[15]P. Vogl, H. P. Hjalmarson, and J. D. Dow, J. Phys. Chem. Solids **44**, 353 (1983). Some parameters have been refit more accuarately to existing data or fit to more recent data in the case of GaSb [T.-C. Chiang and D. E. Eastman, Phys. Rev. B **22**, 2940 (1980)]. These are $V(sa,pc)=V(sc,pa)=4.9617$, $V(s^*a,pc)=V(pa,s^*c)=4.5434$ for Ge; $V(sa,pc)=V(sc,pa)=4.2288$, $V(s^*a,pc)=V(pa,s^*c)=3.9665$ for Sn; $V(sa,pc)=4.2485$, $V(sc,pa)=5.2671$, $E(s^*,a)=8.5014$, $V(s^*a,pc)=4.7525$, $V(pa,s^*c)=4.2547$ for GaAs; $E(s,a)=-7.1256$, $E(p,a)=0.6718$, $E(s,c)=-3.7042$, $E(p,c)=2.7312$, $V(s,s)=-5.9854$, $V(x,x)=1.3546$, $V(x,y)=4.4438$, $V(sa,pc)=5.1693$, $V(sc,pa)=4.4708$, $V(s^*a,pc)=5.1609$, and $V(pa,s^*c)=4.1199$ for GaSb.

[16]We have modified the nearest-neighbor model to include second-neighbor interactions, as discussed for Ge and Si by K. E. Newman and J. D. Dow, Phys. Rev. B **30**, 1929 (1984).

[17]W. A. Harrison and S. Ciraci, Phys. Rev. B **10**, 1516 (1974); W. A. Harrison, *Electronic Structure and the Properties of Solids* (Freeman, San Francisco, 1980).

[18]L. Vegard, Z. Phys. **5**, 17 (1921).

[19]Y. Onodera and Y. Toyozawa, J. Phys. Soc. Jpn. **24**, 341 (1968).

[20]H. Holloway and L. C. Davis, Phys. Rev. Lett. **53**, 830 (1984), have recently suggested that the satisfaction of the Onodera-Toyozawa criterion may not be sufficient to guarantee the validity of a virtual-crystal approximation. We disagree with many of their statements about Ref. 9. The central theoretical arguments of their paper are contradicted by recent experimental results (Ref. 11).

[21]The relative minimum of the conduction band is either at point Γ, or near (or at) points X or L, in the Δ or Λ direction.

[22]D. W. Jenkins, K. E. Newman, and J. D. Dow, J. Appl. Phys. **55**, 3871 (1984).

[23]We are using a notation Γ for s-like states Γ^1, as opposed to p-like states Γ^{15}_c (c denoting the conduction band and v denoting valence band).

[24]Recall that because of ion bombardment during growth, metastable AlP, for example, has more antisite defects and thus should be different from stable equilibrium AlP. This model gives a smaller band gap for metastable III-V compound semiconductors than for the stable III-V compounds. The "magnetization" $M(x;x_c)$ is not unity for $x=0$ in this theory, i.e., the theory predicts a significant concentration of antisite defects.